



**AFRL-RX-WP-JA-2014-0154**

**CORRELATION BETWEEN OPTICAL PROPERTIES  
AND CHEMICAL COMPOSITION OF SPUTTER-  
DEPOSITED GERMANIUM OXIDE (GEOX) FILMS  
(POSTPRINT)**

**Neil R. Murphy, J. G. Jones, and R. Jakubiak  
AFRL/RXAP**

**MARCH 2014  
Interim Report**

**Approved for public release; distribution unlimited.**

*See additional restrictions described on inside pages*

**STINFO COPY**

**© 2014 Elsevier B. V.**

**AIR FORCE RESEARCH LABORATORY  
MATERIALS AND MANUFACTURING DIRECTORATE  
WRIGHT-PATTERSON AIR FORCE BASE, OH 45433-7750  
AIR FORCE MATERIEL COMMAND  
UNITED STATES AIR FORCE**

## NOTICE AND SIGNATURE PAGE

Using Government drawings, specifications, or other data included in this document for any purpose other than Government procurement does not in any way obligate the U.S. Government. The fact that the Government formulated or supplied the drawings, specifications, or other data does not license the holder or any other person or corporation; or convey any rights or permission to manufacture, use, or sell any patented invention that may relate to them.

This report was cleared for public release by the USAF 88th Air Base Wing (88 ABW) Public Affairs Office (PAO) and is available to the general public, including foreign nationals.

Copies may be obtained from the Defense Technical Information Center (DTIC)  
(<http://www.dtic.mil>).

AFRL-RX-WP-JA-2014-0154 HAS BEEN REVIEWED AND IS APPROVED FOR PUBLICATION IN ACCORDANCE WITH ASSIGNED DISTRIBUTION STATEMENT.

*//Signature//*

---

NEIL R. MURPHY  
Photonic Materials Branch  
Functional Materials Division

*//Signature//*

---

CHRISTOPHER D. BREWER, Chief  
Photonic Materials Branch  
Functional Materials Division

*//Signature//*

---

TIMOTHY J. BUNNING, Chief  
Functional Materials Division  
Materials and Manufacturing Directorate

This report is published in the interest of scientific and technical information exchange, and its publication does not constitute the Government's approval or disapproval of its ideas or findings.

# REPORT DOCUMENTATION PAGE

Form Approved  
OMB No. 074-0188

Public reporting burden for this collection of information is estimated to average 1 hour per response, including the time for reviewing instructions, searching existing data sources, gathering and maintaining the data needed, and completing and reviewing this collection of information. Send comments regarding this burden estimate or any other aspect of this collection of information, including suggestions for reducing this burden to Defense, Washington Headquarters Services, Directorate for Information Operations and Reports, 1215 Jefferson Davis Highway, Suite 1204, Arlington, VA 22202-4302. Respondents should be aware that notwithstanding any other provision of law, no person shall be subject to any penalty for failing to comply with a collection of information if it does not display a currently valid OMB control number. PLEASE DO NOT RETURN YOUR FORM TO THE ABOVE ADDRESS.

<b>1. REPORT DATE (DD-MM-YYYY)</b> March 2014		<b>2. REPORT TYPE</b> Interim		<b>3. DATES COVERED (From - To)</b> 06 May 2010 - 17 February 2014	
<b>4. TITLE AND SUBTITLE</b> CORRELATION BETWEEN OPTICAL PROPERTIES AND CHEMICAL COMPOSITION OF SPUTTER-DEPOSITED GERMANIUM OXIDE (GEOX) FILMS (POSTPRINT)				<b>5a. CONTRACT NUMBER</b> In-house	
				<b>5b. GRANT NUMBER</b>	
				<b>5c. PROGRAM ELEMENT NUMBER</b> 62102F	
<b>6. AUTHOR(S)</b> (see back)				<b>5d. PROJECT NUMBER</b> 4348	
				<b>5e. TASK NUMBER</b>	
				<b>5f. WORK UNIT NUMBER</b> X09X	
<b>7. PERFORMING ORGANIZATION NAME(S) AND ADDRESS(ES)</b> (see back)				<b>8. PERFORMING ORGANIZATION REPORT NUMBER</b>	
<b>9. SPONSORING / MONITORING AGENCY NAME(S) AND ADDRESS(ES)</b> Air Force Research Laboratory Materials and Manufacturing Directorate Wright Patterson Air Force Base, OH 45433-7750 Air Force Materiel Command United States Air Force				<b>10. SPONSOR/MONITOR'S ACRONYM(S)</b>  AFRL/RXAP	
				<b>11. SPONSOR/MONITOR'S REPORT NUMBER(S)</b> AFRL-RX-WP-JA-2014-0154	
<b>12. DISTRIBUTION / AVAILABILITY STATEMENT</b> Approved for public release; distribution unlimited. This report contains color.					
<b>13. SUPPLEMENTARY NOTES</b> PA Case Number: 88ABW-2014-0885; Clearance Date: 04 March 2014. Journal article published in Optical Materials 36 (2014) 1177-1182. © 2014 Elsevier B. V. The U.S. Government is joint author of the work and has the right to use, modify, reproduce, release, perform, display or disclose the work. The final publication is available at <a href="http://dx.doi.org/10.1016/j.optmat.2014.02.023">http://dx.doi.org/10.1016/j.optmat.2014.02.023</a> .					
<b>14. ABSTRACT</b> Germanium oxide (GeO <sub>x</sub> ) films were grown on (100) Si substrates by reactive Direct-Current (DC) magnetron sputter-deposition using an elemental Ge target. The effects of oxygen gas fraction, $U = O_2 / (Ar + O_2)$ , on the deposition rate, structure, chemical composition and optical properties of GeO <sub>x</sub> films have been investigated. The chemistry of the films exhibits an evolution from pure Ge to mixed Ge + GeO + GeO <sub>2</sub> and then finally to GeO <sub>2</sub> upon increasing U from 0.00 to 1.00. Grazing incidence X-ray analysis indicates that the GeO <sub>x</sub> films grown were amorphous. The optical properties probed by spectroscopic ellipsometry indicate that the effect of U is significant on the optical constants of the GeO <sub>x</sub> films. The measured index of refraction (n) at a wavelength (k) of 550 nm is 4.67 for films grown without any oxygen, indicating behavior characteristic of semiconducting Ge. The transition from germanium to mixed Ge + GeO + GeO <sub>2</sub> composition is associated with a characteristic decrease in n (k = 550 nm) to 2.62 and occurs at $\Gamma = 0.25$ . Finally n drops to 1.60 for U = 0.50-1.00, where the films become GeO <sub>2</sub> . A detailed correlation between $\Gamma$ , n, k and stoichiometry in DC sputtered GeO <sub>x</sub> films is presented and discussed.					
<b>15. SUBJECT TERMS</b> ellipsometry, reactive sputtering, x-ray photoelectron spectroscopy, germanium oxide					
<b>16. SECURITY CLASSIFICATION OF:</b>			<b>17. LIMITATION OF ABSTRACT</b>  SAR	<b>18. NUMBER OF PAGES</b>  10	<b>19a. NAME OF RESPONSIBLE PERSON (Monitor)</b> Neil R. Murphy
<b>a. REPORT</b> Unclassified	<b>b. ABSTRACT</b> Unclassified	<b>c. THIS PAGE</b> Unclassified			<b>19b. TELEPHONE NUMBER (include area code)</b> (937) 255-1829

## REPORT DOCUMENTATION PAGE Cont'd

### 6. AUTHOR(S)

Neil R. Murphy, J. G. Jones, and R. Jakubiak - Materials and Manufacturing Directorate, Air Force Research Laboratory, Functional Materials Division

J. T. Grant - University of Dayton Research Institute

L. Sun - General Dynamics Information Technology

V. Shutthanandan - Environmental Molecular Sciences Laboratory (EMSL), Pacific Northwest National Laboratory

C. V. Ramana - Mechanical Engineering, University of Texas at El Paso

### 7. PERFORMING ORGANIZATION NAME(S) AND ADDRESS(ES)

AFRL/RXAP

Air Force Research Laboratory

Materials and Manufacturing Directorate

Wright-Patterson Air Force Base, OH 45433-7750

University of Dayton Research Institute

Dayton, Ohio 45469

General Dynamics Information Technology

Dayton, OH 45433

Environmental Molecular Sciences Laboratory (EMSL)

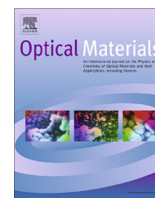
Pacific Northwest National Laboratory (PNNL)

Richland, WA 99352

Department of Mechanical Engineering

University of Texas at El Paso

El Paso, TX 79968



# Correlation between optical properties and chemical composition of sputter-deposited germanium oxide ( $\text{GeO}_x$ ) films



N.R. Murphy<sup>a,\*</sup>, J.T. Grant<sup>b</sup>, L. Sun<sup>a,c</sup>, J.G. Jones<sup>a</sup>, R. Jakubiak<sup>a</sup>, V. Shutthanandan<sup>d</sup>, C.V. Ramana<sup>e</sup>

<sup>a</sup> Materials and Manufacturing Directorate (RX), 3005 Hobson Way, Wright-Patterson Air Force Base (WPAFB), Dayton, OH 45433, USA

<sup>b</sup> Research Institute, University of Dayton, 300 College Park, Dayton, OH 45469, USA

<sup>c</sup> General Dynamics Information Technology, Dayton, OH 45433, USA

<sup>d</sup> Environmental Molecular Sciences Laboratory (EMSL), Pacific Northwest National Laboratory (PNNL), Richland, WA 99352, USA

<sup>e</sup> Department of Mechanical Engineering, University of Texas at El Paso, El Paso, TX 79968, USA

## ARTICLE INFO

### Article history:

Received 30 September 2013

Received in revised form 9 December 2013

Accepted 17 February 2014

Available online 18 March 2014

### Keywords:

Ellipsometry

Reactive sputtering

X-ray photoelectron spectroscopy

Germanium oxide

## ABSTRACT

Germanium oxide ( $\text{GeO}_x$ ) films were grown on (100) Si substrates by reactive Direct-Current (DC) magnetron sputter-deposition using an elemental Ge target. The effects of oxygen gas fraction,  $\Gamma = \text{O}_2/(\text{Ar} + \text{O}_2)$ , on the deposition rate, structure, chemical composition and optical properties of  $\text{GeO}_x$  films have been investigated. The chemistry of the films exhibits an evolution from pure Ge to mixed Ge + GeO +  $\text{GeO}_2$  and then finally to  $\text{GeO}_2$  upon increasing  $\Gamma$  from 0.00 to 1.00. Grazing incidence X-ray analysis indicates that the  $\text{GeO}_x$  films grown were amorphous. The optical properties probed by spectroscopic ellipsometry indicate that the effect of  $\Gamma$  is significant on the optical constants of the  $\text{GeO}_x$  films. The measured index of refraction ( $n$ ) at a wavelength ( $\lambda$ ) of 550 nm is 4.67 for films grown without any oxygen, indicating behavior characteristic of semiconducting Ge. The transition from germanium to mixed Ge + GeO +  $\text{GeO}_2$  composition is associated with a characteristic decrease in  $n$  ( $\lambda = 550$  nm) to 2.62 and occurs at  $\Gamma = 0.25$ . Finally  $n$  drops to 1.60 for  $\Gamma = 0.50$ –1.00, where the films become  $\text{GeO}_2$ . A detailed correlation between  $\Gamma$ ,  $n$ ,  $k$  and stoichiometry in DC sputtered  $\text{GeO}_x$  films is presented and discussed.

Published by Elsevier B.V.

## 1. Introduction

Germanium dioxide ( $\text{GeO}_2$ ) is a versatile, wide band gap material that has been explored in depth due to its promising thermal, optical and electrical properties. Specifically,  $\text{GeO}_2$  is thermally stable, has a high dielectric constant, and exhibits a refractive index that is slightly higher than that of  $\text{SiO}_2$  [1–8]. Applications of thin  $\text{GeO}_2$  films include usage in optical waveguides [1,3,7,9,10], dielectric layers in capacitors [7,11,12], microbolometers [13], and optical filter elements [14–16]. In addition, sub-stoichiometric  $\text{GeO}_2$ , or  $\text{GeO}_x$ , has been studied in depth due to its tendency to form a passivating inter-layer within Ge-based Metal–Oxide–Semiconductor (MOS) devices [17,18], and for its potential in electronic memory storage devices [2,19].

Several methods of depositing  $\text{GeO}_2$  films have been explored previously, including Radio Frequency (RF) magnetron sputtering [1,3,7,8,11,13,20–22], laser ablation [14], sol–gel deposition [2,9,10], reactive thermal evaporation [12,15,23], e-beam evapora-

tion [24], Plasma Enhanced Chemical Vapor Deposition (PECVD) [25], and reactive DC magnetron sputtering [4,14,16,26,27]. Previous works performing in-depth analyses on the chemical, optical and electrical properties of  $\text{GeO}_2$  films were conducted using films with thicknesses ranging from roughly 300 nm to 1.4  $\mu\text{m}$ . Exceptions include experiments by Krupanidhi et al., measuring the electrical properties of 100 nm thick, e-beam deposited  $\text{GeO}_2$  [24], as well as electrical characterization of 3 nm thick  $\text{GeO}_2$  interfacial layers by Murad et al. [12]. Lange et al. and Vega et al. have performed studies concerning the deposition and characterization of  $\text{GeO}_x$  ( $0 \leq x \leq 2$ ) films deposited by DC magnetron sputtering. Analyses conducted by Lange et al. have probed the optical and structural properties of  $\text{GeO}_x$  thin films [4], while studies by Vega et al. were mainly focused on optical characterization [14].

The present work focuses on performing comprehensive optical, chemical and structural characterization of  $\text{GeO}_x$  ( $0 \leq x \leq 2$ ) films, approximately 100 nm thick, grown by DC magnetron sputter-deposition on single crystal (100), n-type silicon wafers. Studies were made to understand the effect of the oxygen gas fraction on the deposition rate, structure, chemistry and optical constants of these very thin  $\text{GeO}_x$  films. The results obtained are presented and discussed in this paper.

\* Corresponding author. Tel.: +1 9372551829.

E-mail address: [neil.murphy.1@us.af.mil](mailto:neil.murphy.1@us.af.mil) (N.R. Murphy).

## 2. Experimental

### 2.1. Fabrication

Germanium oxide ( $\text{GeO}_x$ ) thin films were deposited within a stainless steel vacuum chamber that was evacuated to a pressure of  $4 \times 10^{-7}$  Torr or below. Pumping was accomplished using a turbo-molecular pump in conjunction with a mechanical roughing pump. After reaching the required pressure, research grade  $\text{O}_2$  (99.995%) and Ar (99.999%) were introduced into the chamber using MKS mass flow controllers. The working pressure, controlled via an automated gate valve assembly, was maintained at 5 mTorr. The  $\text{O}_2$  flow rate was varied between 0.0 and 20.0 sccm at increments of 5.0 sccm, and the argon flow rate was adjusted to keep the net flow rate constant at 20.0 sccm. This means that the oxygen gas fraction ( $\Gamma$ ), which is defined as the ratio of the  $\text{O}_2$  gas flow rate to the total ( $\text{O}_2 + \text{Ar}$ ) flow rate, was varied from 0.00 to 1.00 in order to understand its effect on the deposition rate, structure, chemistry and optical properties of the resulting films. The plasma was generated using an Advanced Energy MDX power supply at a power of 50 W DC. A shutter was used to shield the substrate from any spurious droplets caused by arcing at the onset of plasma ignition. The shutter was opened upon achieving a steady-state plasma. A 50 mm germanium sputter target (Plasmaterials, 99.999% purity), attached to a Meivac MAK magnetron sputtering gun, was used as the source material. All films were deposited on prime grade, n-type (100) Si wafers (University Wafer LLC). Wafers were placed on a rotating sample holder (7.7 rpm) located at a distance of 90 mm from the surface of the sputtering target. The substrate temperature was held constant at 100 °C throughout all depositions.

### 2.2. Characterization

$\text{GeO}_x$  films were characterized by performing structural, chemical and optical measurements. Grazing Incidence X-ray Diffraction (GIXRD) and X-ray Reflectivity (XRR) measurements were obtained using a Rigaku SmartLab X-ray diffractometer (see Supplemental Figs. S1 and S2 for information pertaining to XRR density measurement). The GIXRD and XRR measurements were made using  $\text{Cu K}\alpha$  radiation at room temperature.

Ion beam analysis of the  $\text{GeO}_x$  films was performed in order to determine the chemical composition, thickness and elemental depth distribution. Rutherford Backscattering Spectrometry (RBS) experiments were carried out in the accelerator facility at the Environmental Molecular Sciences Laboratory (EMSL) within the Pacific Northwest National Laboratory (PNNL). The RBS experiments were performed at the National Electrostatic Corporation (NEC) RC43 end station. A 2 MeV  $\text{He}^+$  ion beam with a 7° angle of incidence measured from the sample normal was used. The backscattered ions were collected using a silicon barrier detector at a scattering angle of 150°. Composition profiles were determined by comparing SIMNRA [28] computer simulations with the experimental data. The detailed procedure on using this simulation to obtain the stoichiometry and atomic concentration of the films has been discussed elsewhere [29]. In addition to RBS measurements, the chemical valence states of elements, and subsequent stoichiometries, within the films were analyzed using X-ray Photoelectron Spectroscopy (XPS). Most of the XPS measurements were made in a Kratos AXIS Ultra XPS, but a Surface Science Instruments' M-Probe and a Physical Electronics 5700 were used for inert gas sputtering measurements on the films (the ion gun on the Kratos instrument was not operational). All these instruments were equipped with a monochromatic Al  $\text{K}\alpha$  (1486.6 eV) X-ray source, which was used to generate the spectra from all of the deposited

samples. Survey scans were obtained with a high analyzer pass-energy, while high energy resolution spectra, to study the chemical states of Ge, were obtained with a low analyzer pass energy. All high energy resolution spectra were fit using Gaussian–Lorentzian lineshapes, following Shirley background subtraction.

The optical properties of  $\text{GeO}_2$  films were evaluated using Spectroscopic Ellipsometry (SE). Raw data was captured using a J.A. Woollam M2000VI spectroscopic ellipsometer capable of measuring the magnitude ( $\psi$ ) and phase difference ( $\Delta$ ) of polarized light after interaction with the specimen. Data was processed within the CompleteEASE v. 4.7 software package. Raw data was fit with a Cauchy oscillator model in order to estimate the refractive index ( $n$ ), extinction coefficient ( $k$ ), and thickness. However, films with low oxygen content were fit using a general oscillator model with two Tauc–Lorentz oscillators, accounting for the free-carrier absorption associated with amorphous germanium.

## 3. Results and discussion

### 3.1. Deposition rate

The variation of deposition rate with  $\Gamma$  is shown in Fig. 1. The film thickness was determined by three independent methods, SE, XRR and RBS, and was divided by the respective deposition time in order to determine the deposition rate for the various oxygen gas fractions. For RBS, it was assumed that the Ge ( $\Gamma = 0.00$ ) and  $\text{GeO}_2$  ( $\Gamma = 0.5$ –1.00) film densities were the same as bulk Ge and  $\text{GeO}_2$ ; a thickness for  $\Gamma = 0.25$  is not included since the density for this film is unknown. As shown in Fig. 1, the deposition rate from both ellipsometry and XRR data is 23 nm/min when  $\Gamma = 0.00$ . The value obtained from RBS was somewhat lower, most likely due to a lower film density than the bulk value used in the calculation (see Section 3.3). Upon increasing the oxygen gas fraction to 0.25, the deposition rate rose to 47 nm/min. This increased rate is directly related to the larger ion-induced secondary electron emission coefficient of oxide compounds on the surface of the germanium sputter target [30]. The deposition rate remained relatively constant for  $\Gamma = 0.50$ , but dropped precipitously to a value of 7 nm/min for  $\Gamma = 0.75$  (15 sccm  $\text{O}_2$ , 5 sccm Ar), and remained low (5 nm/min) for  $\Gamma = 1.00$ . This reduction in deposition rate is the result of the formation of higher order germanium-oxide

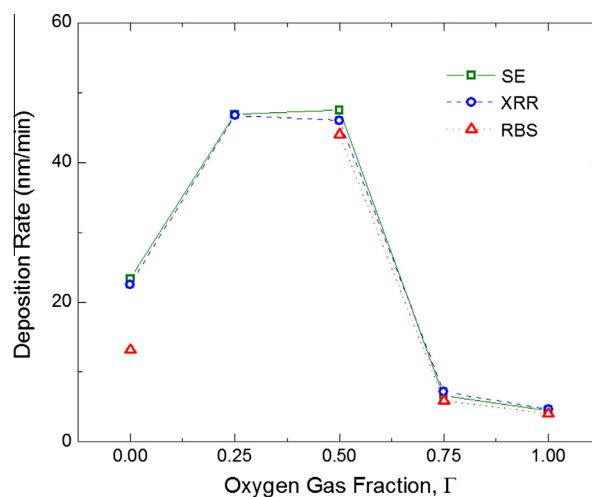


Fig. 1. The dependence of deposition rate of  $\text{GeO}_x$  films with the oxygen gas fraction,  $\Gamma$ . Data are plotted from results using Spectroscopic Ellipsometry (SE), green squares; X-ray Reflectivity (XRR), blue circles; and Rutherford Backscattering Spectrometry (RBS), red triangles. (For interpretation of the references to colour in this figure legend, the reader is referred to the web version of this article.)

compounds on the surface of the target. At a working pressure of 5 mTorr and an oxygen gas fraction of 0.75 and above, the plasma flux can no longer react with the amount of oxygen present within the chamber, leading to oxygen adsorption onto the target surface. The reduction of the deposition rate associated with the formation of germanium-oxide is believed to be a direct result of the decreased sputter yield associated with the covalently bonded compound. The agreement between the deposition rates using the different techniques is remarkably good. The measured film thicknesses and deposition rates using SE, XRR and RBS are listed in Tables I and II, respectively, in the Supplemental Material. Note that the behavior of the deposition rate of  $\text{GeO}_x$  as a function of oxygen partial pressure is similar to those measured in studies conducted by Lange et al. [4] and Vega et al. [14]. However, the maximum deposition rates for stoichiometric  $\text{GeO}_2$ , calculated by Lange et al. and Vega et al., indicate growth rates of 180 nm/min [4] and 15 nm/min [14], respectively, and these largely disparate values are likely the result of their differences in chamber configuration, cathode size, applied power, and working distance.

### 3.2. Crystal structure and morphology

The X-ray diffraction patterns from the  $\text{GeO}_x$  films grown as a function of  $\Gamma$  did not show any features attributable to the films, showing that the  $\text{GeO}_x$  films are all amorphous. The amorphous nature of the films is expected since the substrate temperature during growth is 100 °C. When the substrate temperature is this low, the period of the atomic jump process of adatoms on the substrate surface is very large, and the adsorbed species are unable to diffuse into energetically favorable positions characteristic of a crystalline lattice.

### 3.3. Chemical composition and Ge-valence state

The chemical valence state and surface chemistry of the grown  $\text{GeO}_x$  films was analyzed by XPS. XPS survey spectra from three surfaces are shown in Fig. 2. The survey spectrum from a film grown with  $\Gamma = 1.00$  shows contamination from carbon after exposure to the environment (Fig. 2a) as well as the expected oxygen and germanium transitions. The spectrum after removing carbon by sputtering with 2 keV  $\text{Ne}^+$  ions is shown in Fig. 2b, and a spectrum from a sputtered Ge reference sample is shown in Fig. 2c. The effect of sputtering on the Ge chemistry was studied

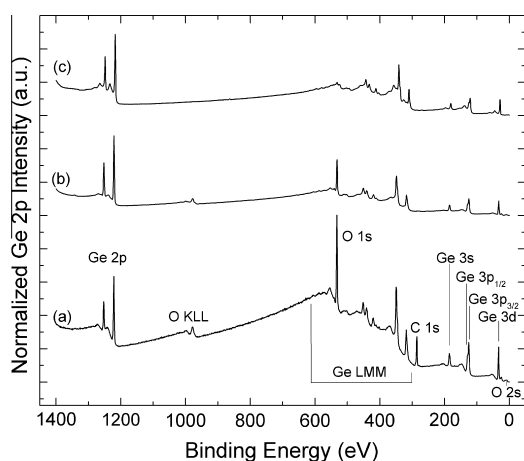


**Fig. 2.** XPS survey scans of (a) as-received  $\text{GeO}_2$  grown at  $\Gamma = 1.00$ , (b) the same film after sputtering with  $\text{Ne}^+$  at 2 keV to remove surface contaminants and (c) a Ge reference sample after sputtering with  $\text{Ne}^+$  at 2 keV to remove surface contaminants. These spectra were taken in the PHI 5700 XPS using an analyzer pass energy of 188 eV.

by comparing high energy resolution 3d spectra from the sputtered samples with the sputtered Ge reference sample. The 3d spectra from a sputtered film grown with  $\Gamma = 1.00$  and the sputtered Ge reference sample are compared in Fig. 3, where the chemical shift between Ge and  $\text{GeO}_2$  can be seen, and also the fact that the  $\text{GeO}_2$  is not reduced on sputtering with 2 keV  $\text{Ne}^+$  ions. This lack of any preferential sputtering means that the composition can also be determined by quantifying the XPS spectrum of the sputtered  $\text{GeO}_2$  film, where it was found that the Ge:O atomic ratio was 0.50 confirming that the film was indeed stoichiometric  $\text{GeO}_2$ .

High resolution XPS spectra were also taken at three different places on all films without any sputtering using the Kratos XPS. (Surface compositions obtained from all the measurements in the Kratos Ultra are compared in Table IV in the Supplemental Material). The energy scale was calibrated using Au and Cu, according to the procedures outlined by the ISO Standard, ISO 15472. Since C was present on the surface of these samples, all of these spectra could be calibrated with respect to the C 1s peak of adventitious carbon at reference energy of 284.6 eV ( $\pm 0.1$  eV). Detailed analysis of the Ge 3d spectra from the sample grown at  $\Gamma = 0.25$ , showed the presence of  $\text{GeO}_2$ , GeO and elemental Ge at the surface, Fig. 4b. Measured binding energies attributed to Ge(0), GeO(II), and  $\text{GeO}_2$ (IV) were 29.0, 30.9, and 32.7 eV, respectively, and agree well with those reported by others using synchrotron radiation [31–33] and traditional XPS [31,33–35]. Some authors [31,34,32] have claimed that Ge(I) and Ge(III) states also exist in oxide films but peaks from these possible states were not needed and have not been included in the peak fits in this work.

Further XPS analysis shows that films deposited for  $\Gamma = 0.00$  were predominantly elemental germanium (29.0 eV) with a small amount of  $\text{GeO}_2$  (32.7 eV) present as a surface oxide layer (Fig. 4a), due to environmental exposure before XPS analysis. This oxide layer was estimated to be about 0.8 nm thick (Fig. S3 and Table III in the Supplemental Material). As mentioned above, at a low oxygen flow,  $\Gamma = 0.25$ , films were comprised of elemental Ge, GeO and a  $\text{GeO}_2$  surface oxide layer (Fig. 4b). Films deposited at higher  $\text{O}_2$  gas fractions ( $\Gamma \geq 0.50$ ) showed the presence of fully stoichiometric  $\text{GeO}_2$ , without the presence of any reduced germanium-oxide species (Fig. 4c). Note the obvious presence of the O 2s peak in Fig. 4b and c.

The RBS spectra of three  $\text{GeO}_x$  films are shown in Fig. 5. The backscattered ions observed are due to scattering by Ge (and O) in the film and Si from the substrate. The scattering from Ge, the

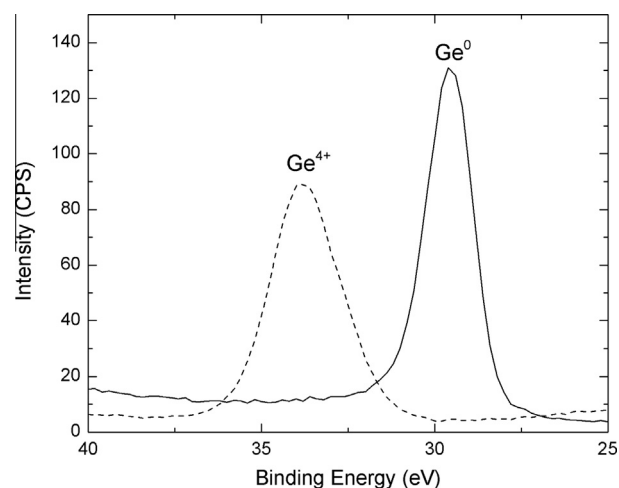


**Fig. 3.** Ge 3d XPS spectra from a Ge reference sample (solid line) and a film grown at  $\Gamma = 1.00$  (dashed line), after sputtering with  $\text{Ne}^+$  at 2 keV to remove surface contaminants. These spectra were taken in the SSI M-Probe using an analyzer pass energy of 100 eV.

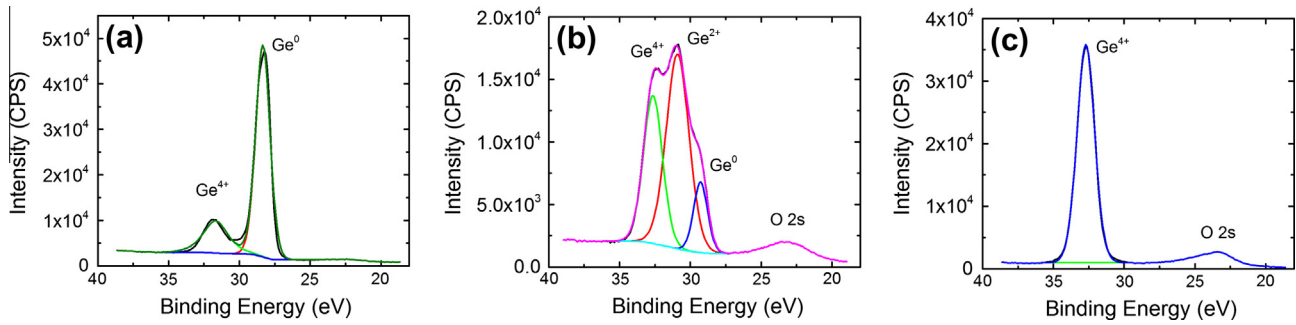


**Fig. 4.** High energy resolution Ge 3d XPS spectra of  $\text{GeO}_x$  films grown at (a)  $\Gamma = 0.00$ , (b)  $\Gamma = 0.25$  and (c)  $\Gamma = 0.50$ . These spectra were acquired in the Kratos Ultra using an analyzer pass energy of 40 eV.

heaviest among the elements present, occurs at the highest back-scattered energies as shown in the RBS spectra (Fig. 5). The measured height and width of this peak is related to the concentration and thickness distribution of Ge atoms in the (oxide) film and serves as a check since known Rutherford scattering cross section and experimental parameters can be used to calculate the composition and areal density of the films [28,29]. The experimental spectra along with the simulated spectra calculated using SIMNRA code are shown in Fig. 5, and it can be seen that the simulated spectra calculated using the experimental parameters are in good agreement with the measured RBS spectra. The film thicknesses can be calculated from the aerial densities if known. Here the Ge and  $\text{GeO}_2$  bulk densities were used to calculate the deposition rate (Fig. 1), except for  $\Gamma = 0.25$  where the film density is not known.

Fig. 5a shows that films grown at  $\Gamma = 0.00$  produce only a Ge peak (and Si from the substrate). No signal due to oxygen is detected, indicating that the film consists entirely of Ge on the Si (100) substrate. The thickness of this Ge film is 63 nm assuming the density of the film is the same as that for bulk Ge. As discussed earlier, the actual thickness of the film is probably larger than this due to loss of density in the film (higher film volume), and this would produce a higher deposition rate than reported in Fig. 1 for the RBS measurement.

For films grown with oxygen, theoretical stoichiometries of germanium compounds namely GeO [Ge(II)] and  $\text{GeO}_2$  [Ge(IV)] were considered. Stoichiometries of GeO and  $\text{GeO}_2$  correspond to an O/Ge atomic ratio of 1 and 2, respectively. The O/Ge atomic ratios calculated from the RBS spectra are 1.04, 2.10, 2.16 and 2.20 for  $\Gamma = 0.25, 0.50, 0.75$  and 1.00, respectively. This shows that the film grown at  $\Gamma = 0.25$  has a significant contribution of GeO (or other reduced species). The values for  $\Gamma = 0.50, 0.75$  and 1.00 are somewhat higher than the expected stoichiometry of the films.

Thus the RBS and XPS analyses together confirm that the films formed at  $\Gamma = 0.00$  are Ge, the transition to mixed oxide composition (Ge + GeO +  $\text{GeO}_2$ ) occurs at  $\Gamma = 0.25$  (Figs. 4b and 5b), and further increase in  $\Gamma$  to 0.50 and above results in the formation of stoichiometric  $\text{GeO}_2$  films.

### 3.4. Optical constants

Optical constants were measured and calculated using a general oscillator model consisting of two Tauc–Lorentz oscillators [36] as well as the Cauchy dispersion equation [37], represented by Eqs. (1)–(3):

$$\epsilon_2(E) = 2nk = \frac{AE_0C(E - E_g)^2}{E^2 - E_0^2 + C^2E^2} \cdot \frac{1}{E} \quad [36] \quad (1)$$

$$n(\lambda) = A + \frac{B}{\lambda^2} + \frac{C}{\lambda^4} \quad [37] \quad (2)$$

$$k(\lambda) = \alpha \exp\left(\beta \left[12, 400 \left(\frac{1}{\lambda} - \frac{1}{\gamma}\right)\right]\right) \quad [37] \quad (3)$$

The latter model (Cauchy dispersion) was used for optically transparent  $\text{GeO}_2$  on account of its negligible extinction coefficient and its decaying refractive index associated with increasing wavelength [37]. The former model (Tauc–Lorentz) was able to account for the free carrier absorption associated with amorphous germanium, allowing for the determination of optical constants for films with minimal oxygen concentration [36]. Note that the  $\text{GeO}_x$  layer was considered to be uniform for all models.

The optical constants, namely index of refraction ( $n$ ) and extinction coefficient ( $k$ ), and their dispersion behavior are shown in Fig. 6a and b, respectively. As expected, films deposited using 0.0 sccm of  $\text{O}_2$  ( $\Gamma = 0.00$ ) have very high  $n$  throughout the measured spectral region (Fig. 6a), reaching a maximum of 5.09 at 810 nm. Additionally, this film is shown to be highly absorbing ( $k > 0$ ) (Fig. 6b), with the extinction coefficient decreasing as it approaches the theoretical band edge of 0.67 eV (1850 nm). At a flow rate of 5 sccm  $\text{O}_2$  ( $\Gamma = 0.25$ ), it can be noted that both  $n$  and  $k$  are lower than for  $\Gamma = 0.00$ . The behavior of the optical dispersion indicates that it consists of a mixture of elemental germanium as well as  $\text{GeO}_2$  and/or GeO. The optical behavior of the film is consistent with the transition regime between an elemental germanium target and a target coated with an oxide compound, as discussed earlier in Section 3.1. The optical properties of the as-deposited  $\text{GeO}_x$  films at  $\Gamma = 0.25$  are indicative of phase separation between oxygen rich  $\text{GeO}_x$  and Ge phases [38]. These findings are further corroborated by the results of the core-level binding energy analysis (XPS), where the films were found to have a mixed composition of Ge + GeO +  $\text{GeO}_2$ .

Films deposited at oxygen flow rates of 20.0, 15.0 and 10.0 sccm of  $\text{O}_2$  ( $\Gamma = 1.00, 0.75, 0.50$ ) displayed optical properties that were almost indistinguishable from one another. These films, all modeled using the Cauchy dispersion layer, displayed a negligible extinction coefficient throughout the measured wavelength region as well as a refractive index that was shown to decrease as a function of increasing wavelength. These films display minimal dispersion, with their respective refractive indices varying from 1.66 to 1.60 within the wavelength region from 380 to 1700 nm. The measured refractive index values for these films are consistent with index values of 1.63–1.58, as reported by Vega et al. for wavelengths ranging from 270 to 870 nm [14].

### 3.5. Structure – optical property correlation

The effect of oxygen fraction during reactive deposition on the chemistry and optical properties of  $\text{GeO}_x$  films can be understood and a processing parameter–chemistry–property relationship can be derived from these results. The semiconducting, amorphous

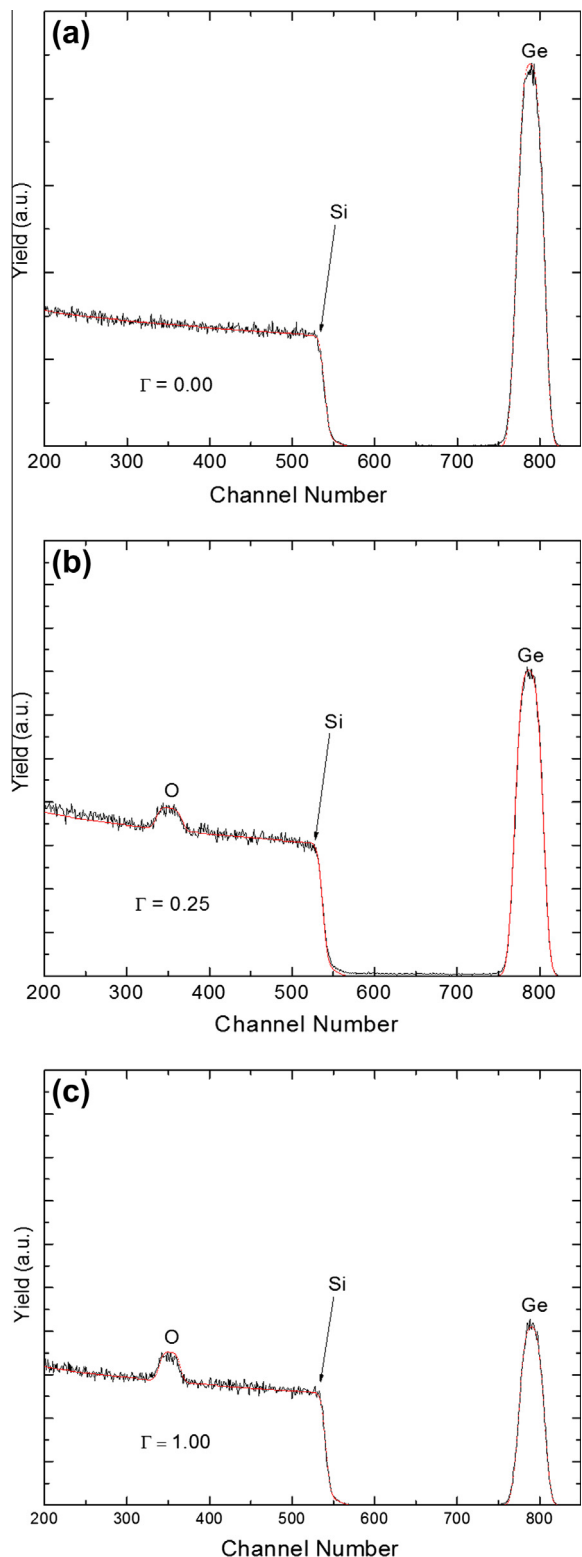


**Fig. 5.** RBS spectra of  $\text{GeO}_x$  films grown at (a)  $\Gamma = 0.00$ , (b)  $\Gamma = 0.25$  and (c)  $\Gamma = 1.00$ . The experimental and simulated spectra are shown for each value of  $\Gamma$ . The energy scale is 2 keV times the channel number.

Ge films, grown at  $\Gamma = 0.00$ , exhibit a high refractive index ( $n$ ) and a high extinction coefficient that decays as the wavelength approaches the theoretical band-edge at 1850 nm. As oxygen is introduced into the gas mixture, Ge–O phases begin to form. Subsequently, oxide phases in the films induce changes in the oxidation state of Ge, which are responsible for the observed

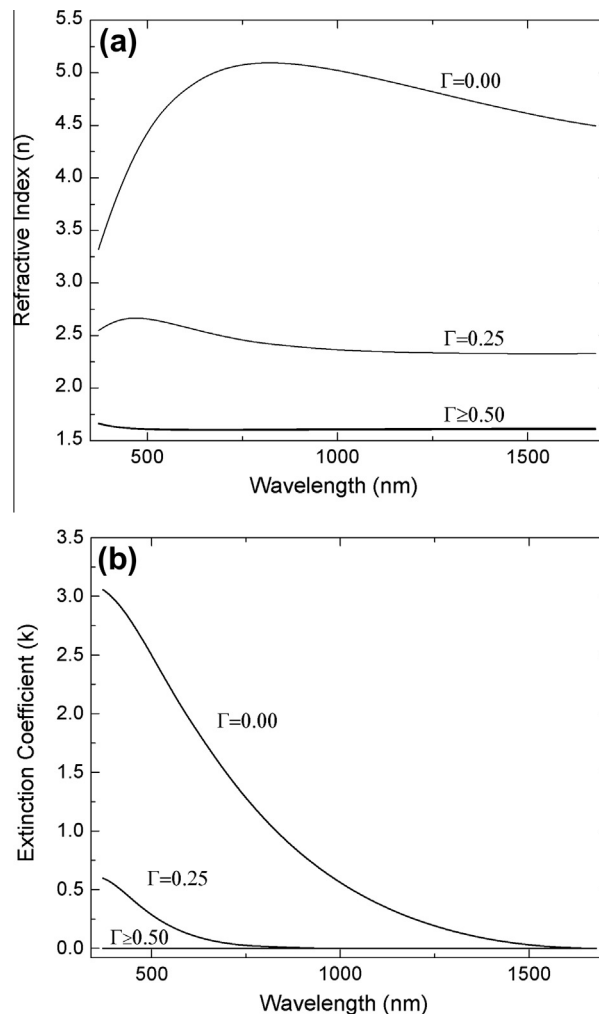


**Fig. 6.** The dispersion profiles for (a) refractive index and (b) extinction coefficient, for  $\text{GeO}_x$  films grown at the different values of  $\Gamma$ .

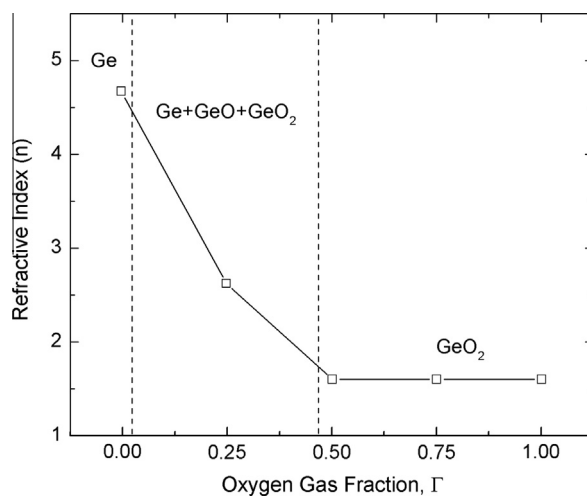


**Fig. 7.** The dependence of refractive index ( $n$ ) on oxygen gas fraction ( $\Gamma$ ) at a wavelength of 550 nm. The approximate regions for different film compositions are shown by the dashed lines.

decrease in the refractive index and extinction coefficient of the films. A minimum  $\text{O}_2$  gas fraction of 0.50 is required to facilitate the formation of fully oxidized ( $\text{GeO}_2$ ) films. Oxygen content less than this value will result in the formation of absorbing, sub-

stoichiometric  $\text{GeO}_x$ , as corroborated by XPS and RBS analyses. Such samples exhibit refractive indices between those reported for pure Ge and  $\text{GeO}_2$  films. Furthermore, the Ge-to- $\text{GeO}_2$  semiconductor-to-insulator transition, shown to occur with increasing oxygen content, serves to further reduce the films' refractive index. The proposed mechanism and correlation between the processing parameters, chemistry and optical behavior is presented in Fig. 7. The aforementioned diagram indicates the three different zones where pure Ge, mixed oxides, and  $\text{GeO}_2$  films can be obtained by controlling the oxygen fraction during deposition. This proposed structure–property correlation is expected to be quite useful for tuning the process parameters to selectively control stoichiometry and subsequent optical behavior of magnetron sputtered Ge–O compounds.

#### 4. Conclusions

Germanium oxide ( $\text{GeO}_x$ ) films were grown by Direct-Current (DC) magnetron sputter-deposition over a wide range of oxygen flow rates. The effect of oxygen gas fraction in the reactive gas mixture significantly affects the chemical composition and optical properties of  $\text{GeO}_x$  films. Structural analysis using X-ray diffraction confirms that all of the  $\text{GeO}_x$  films were amorphous. The chemical state of Ge and the overall stoichiometry of the films exhibit an evolution from pure Ge to a Ge + GeO +  $\text{GeO}_2$  mixed phase and then finally to  $\text{GeO}_2$  with increasing oxygen fraction from 0.00 to 1.00.  $\Gamma$  values of 0.50–1.00 were necessary to obtain stoichiometric  $\text{GeO}_2$  films. Additionally, the effect of  $\Gamma$  is significant on the optical constants of  $\text{GeO}_x$  films. The transition from pure, semiconducting germanium to mixed phase Ge + GeO +  $\text{GeO}_2$  composition was associated with a characteristic decrease in refractive index ( $\lambda = 550$  nm) from 4.67 to 2.62 at  $\Gamma = 0.25$ . Finally the refractive index drops to 1.60 for  $\Gamma = 0.50$ –1.00, for fully stoichiometric  $\text{GeO}_2$  films, corresponding to a valence state of IV. A correlation between the  $\text{O}_2$  gas fraction ( $\Gamma$ ), chemical composition (Ge chemical state) and optical properties ( $n$ ) of DC sputtered  $\text{GeO}_x$  films has been established (Fig. 7). Such a correlation should be useful to select the processing conditions in order to tune the chemical composition, and hence, the optical constants of  $\text{GeO}_x$  films.

#### Acknowledgements

Special thanks to Dr. K.J. Eyink and Dr. H. Koerner of the Air Force Research Laboratory for providing valuable guidance and assistance, as well as the Environmental Molecular Sciences Laboratory (EMSL) located within the Pacific Northwest National Laboratory (PNNL). This work was funded in part by the National Science Foundation (NSF-DMR-0521650) Per DoD instruction 5230.24, this work falls under distribution statement A: Approved for public release; distribution is unlimited 88ABW-2013-3928.

#### Appendix A. Supplementary material

Supplementary data associated with this article can be found, in the online version, at <http://dx.doi.org/10.1016/j.optmat.2014.02.023>.

#### References

- [1] A. Chiasera, C. Macchi, S. Mariuzzi, S. Valligatla, L. Lunelli, C. Pederzoli, D. Rao, A. Somoza, R. Brusa, M. Ferrari, *Opt. Mater. Exp.* 3 (2013) 1561–1570.
- [2] C. Hsu, J. Lin, Y. He, S. Yang, P. Yang, W. Chen, *Thin Solid Films* 519 (2011) 5033–5037.
- [3] V.D. Del Cacho, D.M. da Silva, L.R.P. Kassab, A.L. Siarkowski, N.I. Morimoto, J. Alloys Compd. 509 (Supplement 1) (2011) S434–S437.
- [4] T. Lange, W. Njoroge, H. Weis, M. Beckers, M. Wuttig, *Thin Solid Films* 365 (2000) 82–89.
- [5] C.V. Ramana, G. Carbajal-Franco, R.S. Vemuri, I.B. Troitskaia, S.A. Gromilov, V.V. Atuchin, *Mater. Sci. Eng. B* 174 (2010) 279–284.
- [6] C.V. Ramana, I.B. Troitskaia, S.A. Gromilov, V.V. Atuchin, *Ceram. Int.* 38 (2012) 5251–5255.
- [7] B.G. Segda, C. Caperaa, M. Jacquet, J.P. Besse, *Nucl. Instrum. Methods Phys. Res. Sect. B* 266 (2008) 4829–4836.
- [8] P. Boháč, L. Jastrabík, D. Chvostová, V. Železný, *Vacuum* 41 (1990) 1466–1468.
- [9] D. Chen, B.G. Potter, J.H. Simmons, *J. Non-Cryst. Solids* 178 (1994) 135–147.
- [10] X. Zhang, W. Que, J. Chen, X. Zhang, J. Hu, W. Liu, *Opt. Mater.* 35 (2013) 2556–2560.
- [11] B.G. Segda, M. Jacquet, C. Caopera, G. Baud, J. Pierre Besse, *Nucl. Instrum. Methods Phys. Res. Sect. B* 170 (2000) 105–114.
- [12] S.N.A. Murad, P.T. Baine, D.W. McNeill, S.J.N. Mitchell, B.M. Armstrong, M. Modreanu, G. Hughes, R.K. Chellappan, *Solid-State Electron.* 78 (2012) 136–140.
- [13] M.M. Rana, D.P. Butler, *Thin Solid Films* 516 (2008) 6499–6503.
- [14] F. Vega, J. De Sande, C. Afonso, C. Ortega, J. Siejka, *Appl. Opt.* 33 (1994) 1203–1208.
- [15] J. Beynon, M. El-Samanoudy, E. Short, *J. Mater. Sci.* 23 (1988) 4363–4368.
- [16] J. Beynon, M. El-Samanoudy, S. Al-Ani, *J. Mater. Sci. Lett.* 8 (1989) 786–788.
- [17] A. Dimoulas, D.P. Brunco, S. Ferrari, J.W. Seo, Y. Panayiotatos, A. Sotiropoulos, T. Conard, M. Caymax, S. Spiga, M. Fanciulli, C. Dieker, E.K. Evangelou, S. Galata, M. Houssa, M.M. Heyns, *Thin Solid Films* 515 (2007) 6337–6343.
- [18] J.F. Binder, P. Broqvist, A. Pasquarello, *Appl. Phys. Lett.* 97 (2010). 092903-092903-3.
- [19] J. Beynon, M. El-Samanoudy, *J. Mater. Sci. Lett.* 6 (1987) 1447–1449.
- [20] C. Caperaa, G. Baud, J.P. Besse, P. Bondot, P. Fessler, M. Jacquet, *Mater. Res. Bull.* 24 (1989) 1361–1367.
- [21] T. Minami, T. Nakatani, T. Miyata, T. Shirai, *Surf. Coat. Technol.* 146–147 (2001) 508–512.
- [22] N. Terakado, K. Tanaka, *J. Non-Cryst. Solids* 351 (2005) 54–60.
- [23] B. Rai, *Phys. Status Solidi A* 100 (1987) K189–K193.
- [24] S.B. Krupanidhi, M. Sayer, A. Mansingh, *Thin Solid Films* 113 (1984) 173–184.
- [25] S. Reich, H. Suhr, B. Waimer, *Thin Solid Films* 189 (1990) 293–302.
- [26] A. Shabalov, M. Feldman, *Phys. Status Solidi A* 83 (1984) K11–K14.
- [27] L. Pajasová, D. Chvostová, L. Jastrabík, J. Poláček, *J. Non-Cryst. Solids* 182 (1995) 286–292.
- [28] M. Mayer, *SIMNRA User's Guide*, 1997.
- [29] V. Mudavakkat, V. Atuchin, V. Kruchinin, A. Kayani, C. Ramana, *Opt. Mater.* 34 (2012) 893–900.
- [30] S. Mohamed, O. Kappertz, J. Ngaruiya, T. Leervad Pedersen, R. Drese, M. Wuttig, *Thin Solid Films* 429 (2003) 135–143.
- [31] A. Molle, M. Bhuiyan, N. Kabir, G. Tallarida, M. Fanciulli, *Appl. Phys. Lett.* 89 (2006). 083504-083504-3.
- [32] D. Schmeisser, R. Schnell, A. Bogen, F. Himpfel, D. Rieger, G. Landgren, J. Morar, *Surf. Sci.* 172 (1986) 455–465.
- [33] N. Tabet, M. Faiz, N. Hamdan, Z. Hussain, *Surf. Sci.* 523 (2003) 68–72.
- [34] K. Prabhakaran, T. Ogino, *Surf. Sci.* 325 (1995) 263–271.
- [35] J.S. Hovis, R.J. Hamers, C.M. Greenlief, *Surf. Sci.* 440 (1999) L815–L819.
- [36] G. Jellison, F. Modine, *Appl. Phys. Lett.* 69 (1996) 371–373.
- [37] Y.C. Liu, J.H. Hsieh, S.K. Tung, *Thin Solid Films* 510 (2006) 32–38.
- [38] D. Ristić, M. Ivanda, G. Speranza, Z. Siketić, I. Bogdanović-Radović, M. Marciuš, M. Ristić, O. Gamulin, S. Musić, K. Furić, *J. Phys. Chem. C* 116 (2012) 10039–10047.